A REAL TIME SPEED MODULATION SYSTEM TO IMPROVE OPERATIONAL ABILITY OF AUTONOMOUS PLANING CRAFT IN A SEAWAY

(DOI No: 10.3940/rina.ijme.2020.a4.635)

H Allaka, A Levy, D Levy, T Triebitz and **M Groper,** The Hatter Department of Marine Technologies, Leon H. Charney School of Marine Sciences, University of Haifa, Israel

KEY DATES: Submitted: 16/03/2020 Final acceptance: 04/11/2020 Published: 04/12/2020

SUMMARY

This study focuses on developing a control system to enhance the seaworthiness of Autonomous high-speed Planing Crafts (APCs). APCs operating at high-speed in a seaway encounter very high vertical accelerations which pose a hazard to payload and crafts' structural integrity. Therefore, for safety operation of APCs in a seaway it is proposed to employ a system termed vision-aided speed modulation system (VSMS). The proposed VSMS employs an embedded analytical tool termed Motion Assessment of Planing Craft in a Seaway (MAPCS) for the prediction of vertical accelerations and angular velocities, the APC might encounter in the incoming waves. As a response to the MAPCS predicted values the VSMS speed setting module modulates the craft's forward speed. All modules of the VSMS are presented together with their validation and system's preliminary operational results. It is concluded that VSMS might be an essential tool to considerably enhance the operational ability of APCs.

NOMENCLATURE

$\theta_{cg}, \ddot{\theta}_{cg}$	Pitch angle and acceleration at CG
D	Frictional Drag Force [N]
EKF	Extended Kalman Filter
H_S	Spectral significant wave height [m]
$H_{1/3}$	One third wave height [m]
H_{max}	Maximum wave height [m]
I	Mass moment of inertia in pitch [kg.m2]
PID	Proportional, Integral, Differential
T	Thrust Force [N]
T_P	Peak period [sec]
W	Weight of the ship [N]
$\ddot{x}_{cg}, \ddot{z}_{cg}$	Surge and Heave accelerations at CG
x_a, x_b, x_d, x_t	Moment arm of hydrodynamic, hydrostatic, drag and thrust force [m]

1. INTRODUCTION

The study of autonomous navigation of marine crafts in general and APCs in particular is a fast developing research field, but most ongoing studies focus on autonomous navigation and path planing algorithms. Those are mainly based on machine processing of nautical charts combined with some collision and obstacles avoidance systems (Campbell et al. 2013; Larson et al. 2006; Heidarsson & Sukhatme 2011; Blaich et al. 2015; Zhuang et al. 2016; Multi-Purpose USV & Protector n.d.; Moe & Pettersen 2017; Hermann et al. 2015; Tripp & Daltry 2017; Wang et al. 2011; El-Gaaly et al. 2013). Currently, to the best of our knowledge, the existing autonomous navigation systems cannot address the seaworthiness challenges posed to APCs when operating in real sea conditions. While in manned operation the skipper can, to some degree, limit the accelerations by adjusting the craft's speed and course in response to its behavior as he feels and expects, in an unmanned mode the speed and course are predefined in the mission plan and autonomous adjustment as a response to the craft's behavior to incoming waves is typically not provided. In this work it is considered that the prediction and estimation, in real time, of expected vertical acceleration and angular velocity in a seaway the APC might develop, and a control algorithms embedded in the crafts' autonomous navigation systems to limit those by automatically adjusting the APC forward speed are an essential need to ensure safe operation of APCs. Consequently, the ability for autonomous speed setting in response to the incoming waves is vital (Allaka et al. 2018). Therefore, a computational model-based system, integrated into the APC navigation system, which can determine in real time the expected acceleration and angular motion of the craft based on knowledge of the characteristics of incoming waves, is developed. The system presented, based on the real-time motion computational model MAPCS and visual and inertial sensors, will assist the craft's autonomous navigation system by adjusting the craft's momentary speed in a seaway to limit vertical acceleration and to preserve its structure and payload safety and integrity. The incoming waves characteristics provided as an input to the MAPCS in real time by a dedicated vision system was also developed in the frame of this research. Figure 1 presents the general configuration of the VSMS framework.

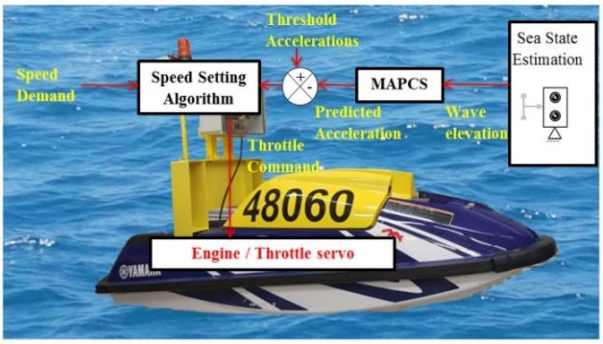

Figure 1. APC with VSMS framework

This includes the following components:

a. Estimation of the characteristics (height and frequency) of incoming waves is essential for APC navigation. This data is obtained from the sea state estimation system installed onboard the craft and equipped with visual and inertial sensors.
b. Based on the incoming waves and craft's characteristics, the MAPCS (Allaka 2017; Allaka & Groper 2020) predicts the vertical acceleration the APC might develop as a function of the forward speed.
c. The speed setting algorithm modulates the speed of the APC as a function of the predefined acceleration threshold and the MAPCS predicted acceleration values and sends a corrective throttle command setting accordingly.

This paper is structured as follows: A brief overview of existing navigation systems for autonomous surface crafts and sea state estimation methodologies is presented in section 2. The principles of the VSMS and a brief overview of MAPCS are presented in section 3. APCs configuration with vision system and its performance accuracy is presented in section 4. The wave elevation estimation system and its validation in real sea experiments is presented in section 5. The testing of the VSMS and its results are discussed in section 6. Finally the conclusions are presented in section 7.

2. EXISTING NAVIGATION SYSTEMS OF AUTONOMOUS SURFACE CRAFTS

Existing autonomous surface platforms that offer autonomous navigation capabilities developed for both research, commercial and military applications (Campbell et al. 2013; Larson et al. 2006; Heidarsson & Sukhatme 2011; Blaich et al. 2015; Zhuang et al. 2016; Multi-Purpose USV & Protector n.d.; Moe & Pettersen 2017; Hermann et al. 2015; Tripp & Daltry 2017; Wang et al. 2011; El-Gaaly et al. 2013) are typically equipped with the following:

a. An auto pilot system which allows operators to define a mission plan by demarcating lines, orbits or waypoints and speeds in the segments between waypoints using a dedicated GUI and existing, often system embedded, nautical charts. The auto pilot system controls the craft course and speed to follow this predefined plan.
b. An obstacle avoidance system (OAS), which makes deliberate, real time, navigational decisions to avoid collisions with other crafts or floating objects.
c. An over-the-horizon communication system, for remote control operations (takeover) and telemetry beyond line of sight distances.

Although several authors (Wang et al. 2011; Hermann et al. 2015; El-Gaaly et al. 2013; Heidarsson & Sukhatme 2011; Tripp & Daltry 2017; Campbell et al. 2012; Larson et al. 2006) developed obstacle avoidance systems for unmanned surface crafts using either radar or vision technologies or a combination of both, to the best of our knowledge, no study describing an autonomous navigation system for unmanned surface crafts that includes a sub-system to estimate sea state and modulate vehicle speed accordingly to ensure safety has been published.

2.1 SEA STATE ESTIMATION

The routinely employed classical method to attain sea state figures is to process motion measurements obtained from traditional wave rider moored buoys deployed at fixed locations to obtain the waves spectrum and, consequently, the sea state. In the context of this work, to enhance the navigation and safe operation of APCs in a seaway, accurate estimation of the sea state in front of craft is essential. Thus, onboard sensors whose data is processed in real time to estimate sea state are investigated here.

There are only a limited number of works where onboard sensors such as Inertial Measuring Units (IMUs) (Nielsen et al. 2017; Rosén et al. 2017; Nielsen et al. 2016), radars (Jian Cui et al. 2017) and vision systems (Bergamasco et al. 2017; Corgnati et al. 2015) were used to measure in situ sea state from sailing vessels.

Several authors (Nielsen et al. 2017; Rosén et al. 2017; Nielsen et al. 2016) have worked on sea state estimation using vessel's motion measurements as input. A key assumption in these works is that in low to moderate sea states, the wave-induced six degrees-of-freedom motion of a vessel are linear with the incident waves. This linear assumption between the exciting waves and the associated vessel's responses facilitates the use of response amplitude operators (RAOs), which, once reversely used, express how the measured vessels response spectrum is transferred into wave spectrum.

Use of this approach in the context of this work is unsatisfactory because of two main limitations:

1) As the behavior of high-speed planing crafts in a seaway is highly non-linear, the use of RAOs in their classical linear sense may result in insufficiently accurate results.
2) As the intention of this work is to modulate the craft's speed in response to incoming waves, it is advantageous to estimate their height at a distance, in the undisturbed sea surface in front of the craft.

Cui (Jian Cui et al. 2017) employed an onboard radar system to measure waves height. Specifically, the systems comprised two radar units, a long-range radar used to detect sea surface objects a few kilometers away from the craft and a short-range frequency modulated continuous wave radar to detect nearby obstacles. It was said that this short-range radar was employed in the estimation of the wave's height in front of the craft and consequently enhance the safe navigation of the

unmanned surface vehicle. Experimental results obtained from the short-range radar system from both wave tank and real sea tests were presented. The author concluded that the radar system was capable of estimating the sea state; however, no comparison with a validated wave estimation system was presented. Also, the author did not elaborate on how exactly the wave estimation as obtained from the radar system was utilized to enhance the safe navigation of crafts.

Few authors (Bergamasco et al. 2017; Corgnati et al. 2015) employed stereo vision systems to estimate sea state. Corgnati et al. (Corgnati et al. 2015) employed a passive stereo vision system for real-time evaluation of sea wave characteristics, e.g., period and significant wave height, using a 3D model of the sea surface. The 3D reconstruction was based on solving correspondence problems (stereo matching) when creating a point cloud. The solution for wave estimation was based on spatial measurements and, therefore, a full 3D reconstruction was needed. The method relies on calculating wavelength; thus, the images must contain at least two waves and, accordingly, have to be taken from a significant height. For the goals of the present work, only wave elevation data in the time domain at a certain distance from the camera is required, eliminating the need for a complete 3D reconstruction of the captured images. Therefore, a computational fast and reliable methodology to obtain wave elevation at a certain distance in front the camera was developed and employed in this work and is described in the following sections.

3. VISION AIDED SPEED MODULATION SYSTEM (VSMS) OVERVIEW

The VSMS configuration schematically presented in Figure 2 comprises a vision system equipped with an, in house developed, stabilized stereo camera arrangement used to capture the state of the approaching sea in front of the craft. The stereo camera is stabilized in two axes: roll, and pitch. The vision system algorithm computes the elevation of the incoming waves at a constant, predefined distance ahead of the craft in the camera's reference frame by reconstruction using stereo imaging. Thereafter, the computed wave elevation data is heave-compensated using heave position data as recorded by an IMU installed on the stabilized stereo camera frame to obtain the wave elevation in the inertial frame. Although the obtained momentary wave elevation in front of the APC will not be exactly the momentary wave elevation that the craft will actually encounter as the waves propagates, in a statistical fashion and based on the high speed of advance of the planing craft, wave propagation is ignored. Consequently, the vision system obtained wave elevation is considered as the one the craft will encounter, and the two momentary sea elevations are treated as different realizations of the same sea state. Thus, the incoming seaway wave elevation data provided by the vision system algorithm and the actual velocity of the APC are fed as input to the MAPCS. Based on this input, the MAPCS predicts the vertical acceleration and pitch angular velocity of the APC. Then, the predicted acceleration values are compared with the threshold/permissible value. The difference between the predicted and threshold acceleration values are provided as input to the speed setting algorithm. If the predicted acceleration values exceed the threshold limit, the speed setting algorithm will momentarily and in real time reduce the actual speed demand based on a simplified linear algorithm. The updated speed demand is sent in real time to the autopilot system, which provides it as an updated value to the throttle command.

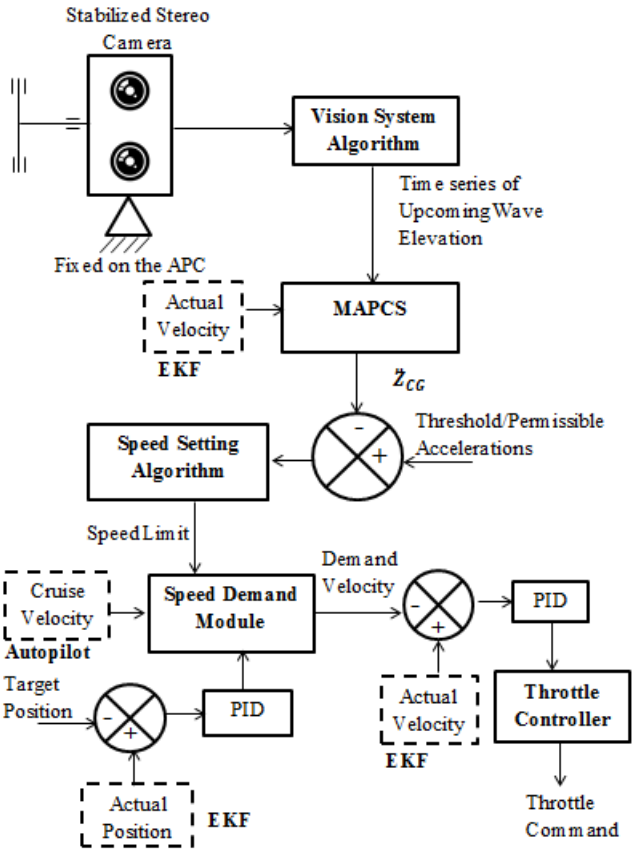

Figure 2. Vision Aided Speed Modulation System

3.1 MAPCS MODEL OVERVIEW

The MAPCS model used in the VSMS to estimate planing crafts' vertical acceleration and angular pitch velocity was developed by the authors following the work of Zarnick (Zarnick 1978) and by incorporating the pressure correction (Garme 2005) and modified added-mass theories (Payne 1994). The craft is modelled as a series of strips or impacting wedges. MAPCS is capable to predict the craft's motions in the longitudinal plane (surge, heave and pitch) when operating in head or following seas.

The expressions for the surge x_{CG}, heave z_{CG}, and pitch θ_{CG} (where CG refers to the craft's center of gravity) directions are presented in expression (1):

$$\begin{aligned} M\ddot{x}_{CG} &= T\cos\theta_{CG} - F_{dyn}\sin\theta_{CG} - D\cos\theta_{CG} \\ M\ddot{z}_{CG} &= -T\sin\theta_{CG} - F_{dyn}\cos\theta_{CG} - F_{sta} + D\sin\theta_{CG} + W \\ I\ddot{\theta}_{CG} &= Tx_t + F_{dyn}x_a + F_{sta}x_b - Dx_d \end{aligned} \quad (1)$$

The total hydromechanical normal force acting on the planing craft is the vectorial summation of the hydrodynamic lift force F_{dyn} and the hydrostatic lift force F_{sta}. When a wave impinges on the hull, the immersion of hull volume changes along the length of the craft altering both the hydrodynamic forces F_{dyn} and hydrostatic forces F_{sta} as shown in Figure 3.

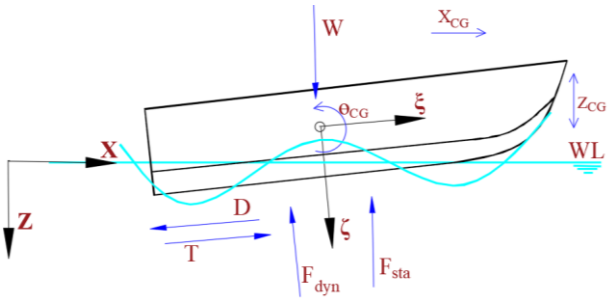

Figure 3. Forces acting on a planing craft in waves

The solution of the nonlinear set of ODEs (1) allows the computation of the craft's motion in the longitudinal plane and in the time domain.

The detailed development of the MAPCS model, its validation and verification are detailed in (Allaka 2017; Allaka & Groper 2020; Allaka et al. 2018).

4. APC CONFIGURATION WITH VISION SENSORS

To facilitate autonomous speed modulation in a seaway, a vision system was developed and installed onboard the APC. Currently, the vision system uses a stabilized stereo camera system which facilitates sea state estimation. The present system can estimate wave elevation up to 50 [m] in front of the craft improving our previous version ZED based stereo camera setup which was limited to 20 [m] (Allaka et al. 2019).

4.1 STABILIZATION OF THE VISION SYSTEM AND ITS VALIDATION

The VSMS requires a stream of incoming wave elevation data in the time domain. Ensuring accuracy of the wave elevation measurements is of significant importance to the correct operation of the system and optimal performance of the APC. To this end, it was decided to develop, in-house, a robust and stabilized mount for the vision system. To stabilize the stereo camera in two axes (roll, and pitch), a gimbal frame made of carbon fiber plates and tubes was developed. Two brushless motors were installed onto the gimbal frame, one for stabilizing the roll axis and the other for stabilizing the pitch axis, as presented in Figure 5. A BGC 32-bit extended brushless gimbal controller was used to stabilize the system. The controller's proportional integral differential (PID) parameters were fine-tuned for faster response and perfect stabilization.

To get an estimation of how effective the in-house developed stabilization system performs when the APC operates at planing speeds in a real seaway, an IMU was mounted on the vision system camera to record its linear and angular motion, with an additional IMU installed inside the vision system cabinet on an unstabilized frame. A comparison was made between these two IMUs readings. It was observed that the stabilization system performs well but there are few events where it fails to stabilize. Those are high impact slams the craft encountered when operating in high seas and at planing speeds. The effect of those events on the computed wave elevation data is numerically filtered (Allaka et al. 2019).

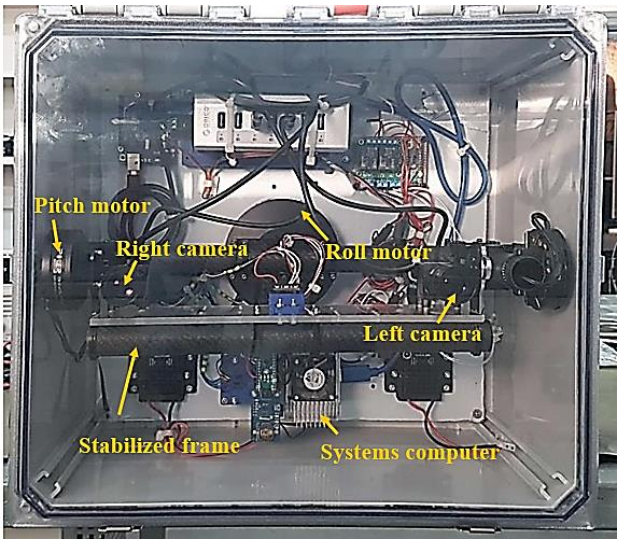

Figure 4. Stabilized vision system setup

5. WAVE ELEVATION ESTIMATION FROM VISION AND INERTIAL SENSORS

The passive stereo vision system mounted on the craft is stabilized in roll and pitch axes (roll and tilt)). It will, however, be displaced in the heave direction (along the Z-axis) in response to the craft motion in a seaway; this non-compensated motion will cause a deviation in the computed waves' elevation. To take account of this motion, an additional IMU was installed on the stereo vision camera to estimate its exact heave position. The employed coordinate systems are shown in Figure 5: Stabilized, IMU coordinates $(O_{imu(s)}, x_{imu(s)}, y_{imu(s)}, z_{imu(s)})$, stereo system left $(O_{CL}, x_{CL}, y_{CL}, z_{CL})$, right $(O_{CR}, x_{CR}, y_{CR}, z_{CR})$ and the

actual wave elevation coordinates (O_i, x_i, y_i, z_i). The wave elevation of the vision system is processed in the camera's left frame $(O_{CL}, x_{CL}, y_{CL}, z_{CL})$; thus, the stabilized IMU $(O_{imu(s)}, x_{imu(s)}, y_{imu(s)}, z_{imu(s)})$ was mounted in close proximity to the camera's left frame and the origins were considered to coincide.

Figure 6 presents a sample reconstruction of the wave elevation time history in the camera frame $(O_{CL}, x_{CL}, y_{CL}, z_{CL})$, red curve, the heave displacement of the stereo vision camera in the stabilized IMU frame $(O_{imu(s)}, x_{imu(s)}, y_{imu(s)}, z_{imu(s)})$, blue curve and the heave compensated wave elevation reconstruction, in the inertial frame(O_i, x_i, y_i, z_i), green curve.

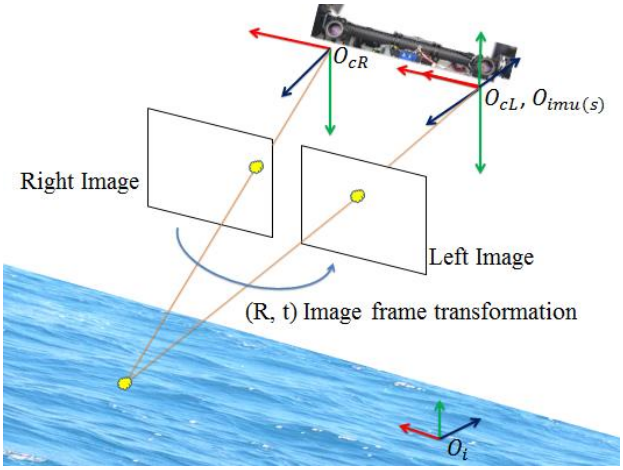

Figure 5. The four coordinate systems involved in the vision system

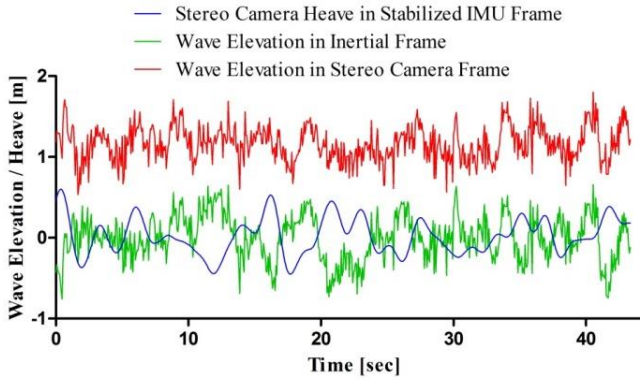

Figure 6. Wave elevation and system heave displacement time history

5.1 VALIDATION OF WAVE ELEVATION AS OBTAINED FROM THE VISION SYSTEM IN REAL SEAS

To validate and confirm the performance of the vision system in a real operational scenario sea experiments were performed with the system installed onboard a manned 6.5m in length planing craft operated at planing speeds in real seas. To verify the accuracy of the wave elevation data as obtained from the vision system, our in-house developed wave buoy (Farber et al. 2019) was deployed in the region of the sea experiment.

Based on the stereo imaging, 3D reconstruction of the scene (except for occlusions) was performed in batch processing. Both the intrinsic and extrinsic parameters of the stereo cameras as supplied by the manufacturer were used. The next step was to find matching points in both images in order to triangulate the real-world data points. This task is quite difficult due to similarity of features in the images. To find dense matching, an epic flow algorithm (Revaud et al. 2015) was employed and applied in a bi-directional manner: from the left image to the right and vice-versa. A match was considered to be valid only for pixels that had an end-point-error of 3 pixels or less for images with resolution of 1920x1080 pixels (HD). The point cloud was validated by measuring the size of the wave amplitude from the data. The last step was to decide at which distance from the camera the water surface has to be observed.

The vision system captured recordings were batch processed to obtain wave elevation at three different distances in front of the craft. The wave elevation data compensated for heave and the spectral and time domain parameters of the wave records for these distances as obtained from the vision system were statistically compared against data collected by our in-house developed buoy and against a standard wave buoy operated by the Coastal and Marine Research Institute - CAMERI (CAMERI - Real Time Wave Measurements Haifa 2020) and located in a close vicinity to the experimental site and is presented in Figure 7.

In this figure a comparison of the wave elevation spectral parameters, i.e. spectral significant wave height (H_S) and peak wave period (T_P) as obtained from the stereo vision system vs. our wave buoy and vs. the standard CAMERI wave buoy is presented.

The abscissa represents the distance in front of the craft (where the sea state parameters were evaluated) and the results obtained from the employed wave buoys. The ordinate represents the value of the estimated parameters.

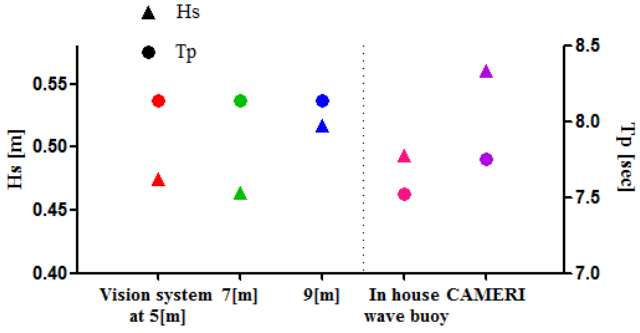

Figure 7. Wave elevation spectral parameter comparison

As can be observed at the day of the experiment the significant wave height as estimated using the vision system data was 0.47m, 0.46m and 0.52m at distances of 5m, 7m and 9m in front the craft accordingly. At the same sea realization the significant wave height as obtained using our wave buoy was 0.49m and the CAMERI buoy recorded a significant wave height of 0.55m. The peak period as estimated using the data provided by the vision system was 8.2s for all three distances where the data collected by our buoy provided a peak period equal to 7.7s and CAMERI 8.3s.

Based on this comparison (and additional performed but not presented here) it seems that the waves spectral (H_S and T_P) and time domain ($H_{1/3}$, H_{max}) sea state parameters as obtained using the developed stereo vision system operated in a real operational scenario shows a fair correlation with the values obtained from our self-developed buoy and with the data obtained from the standard wave buoy operated by CAMERI (CAMERI - Real Time Wave Measurements Haifa 2020).

5.2 WAVE ELEVATION FROM THE UPGRADED VISION SYSTEM

The vision system employed here is an improved and upgraded version of our previous ZED based stereo camera system (Allaka et al. 2019) replaced with IDS imaging - UI - 3260CP rev.2 cameras equipped with Tamron 1/1.2" C 35mm (fixed focal length) lenses.

To verify the accuracy of the upgraded vision system measured elevation data, an experiment was performed by placing a ground truth object at a certain distance and at a known height relative to the stereo camera set-up. The frames were captured at a frequency of 1 HZ using the stereo camera. Based on the stereo imaging, reconstruction of the scene was performed in sequential processing. Figure 8 presents the height of the reconstructed ground truth object at a distance of 10.5 [m] from the stereo camera. The height of the ground truth object was measured to be equal to a height of 0.17 [m] corresponding perfectly with the manual measurement of 0.17 [m] .The blue points indicated by arrow in Figure 8 are the pixels that were considered as pixels that denote the ground truth object.

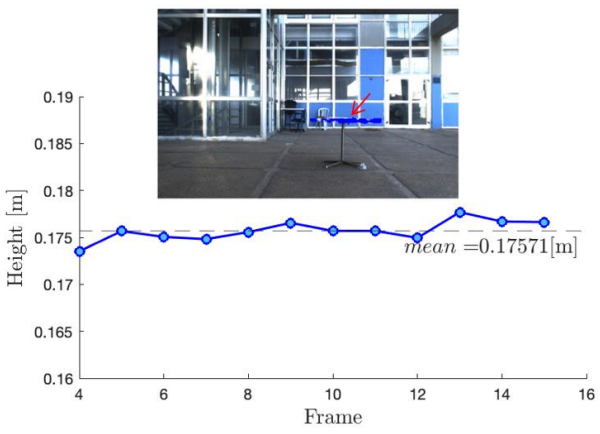

Figure 8. Ground truth validation of the stereo camera set-up

Further, an experiment was conducted near the shore to measure wave elevation in real seas, here the frames were captured at a frequency of 5 Hz. Figure 8 shows the wave elevation at a distance of 47 [m] in front of the camera. Similar to Figure 8, the blue points indicated by arrow in Figure 9 are the pixels that were considered as pixels that denote the upcoming wave at a prescribed distance from the stereo camera.

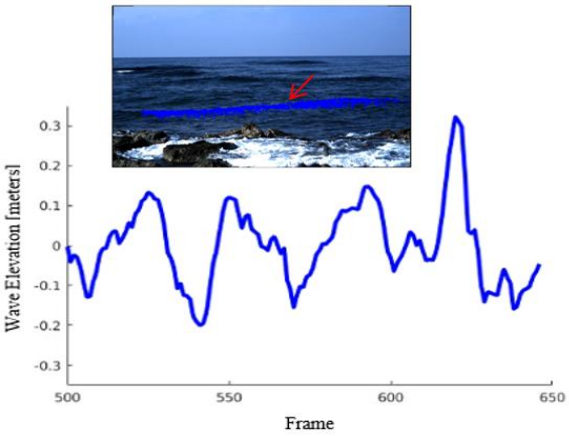

Figure 9. Wave elevation at a distance of 47m from the camera

6. TESTING OF VSMS SYSTEM

The performance of the complete VSMS system performance was examined offline in a simulated MATLAB/SIMULINK environment using the experimental real seas' wave elevation data as captured by the vision sensors and the previously developed MAPCS model.

The VSMS algorithm and conditions were set as follows:

1. As soon as the APC is operated the vision sensors begin accumulating wave data for the first 20 seconds while the VSMS remains idle, with the craft's speed of advance setting equals to the preset setting.
2. Once 20 seconds of wave data is accumulated, the VSMS system starts operating, with the MAPCS computing predicted vertical acceleration values each time the APC is operated at planing speeds, i.e. $F_r \geq 0.8$.
3. In planing speeds operation, the predicted vertical acceleration data is fed to the speed setting algorithm where the vertical acceleration peaks are compared against the user-defined threshold values and if the former exceed the threshold, through an iterative process, an appropriate speed limit is computed. For the offline simulation purpose it was decided to update the APC speed setting every 20s only. In real sea experiments to follow, based on the real time computational time, the behavior of the APC propulsion plant and its reaction to speed changes, the update rate of the speed setting will be tuned.

4. This newly computed speed limit overrides the preset speed setting and the throttle is modulated accordingly through a PID controller.
5. As long as the APC is at planing speeds, the VSMS will continue its operation and compute speed limits to modulate the preset on-route speed as originally dictated in the mission planner.

Figure 10 presents the VSMS Simulink environment model where blocks of the craft geometry, the sea state and the state space initial conditions were fed as input to the MAPCS model. The sea state data provided as input was based on simulated data from the vision system at a distance of 50m in front of the APC.

The sea state data from the vision system is transformed into a set of n-regular waves using Fourier transform. Based on this input, the MAPCS model predicted the vertical acceleration peaks, which were fed to the iterative speed setting algorithm, and a speed limit was obtained. This new speed limit overrode the preset surge velocity in the state vector provided as input to the MAPCS model. The MAPCS model uses ODE45 variable step solver for the simulations.

Figure 11 presents a comparison of simulated vertical acceleration encountered by our experimental APC, 2.24m in length without an active VSMS (Figure 11 (b)) and with the VSMS (Figure 11(c)) active for the same wave elevation time history (Figure 11(a)).

The preset on-route speed was set to 12 m/sec $(F_r = 2.5)$. Figure 11(b) presents the predicted craft's vertical acceleration (in green) without the intervention of the VSMS. The acceleration threshold is marked with a dotted red line (set at 60 m/s^2) and the actual speed of the craft in blue. As the VSMS is not active, the actual speed of the craft equals the preset on-route speed.

Figure 11(c) presents the predicted craft's vertical acceleration (in green) with the intervention of the VSMS, the acceleration threshold again marked with a dotted red line (set at 60 m/s2) and the actual speed of the craft (in blue). It can be observed that when the VSMS is engaged, the craft's speed is modulated as dictated by the speed setting algorithm.

Comparing the vertical acceleration in Figures 11(b) and 11(c), when no VSMS system is employed (Figure 11(b)), the vertical acceleration peaks cross the threshold acceleration limit often with a very high magnitude. In contrast, when the VSMS system is engaged (Figure 11(c)), the speed modulation causes a drastic reduction in encountered vertical acceleration peaks and the vertical acceleration peaks rarely crossed the threshold acceleration limit.

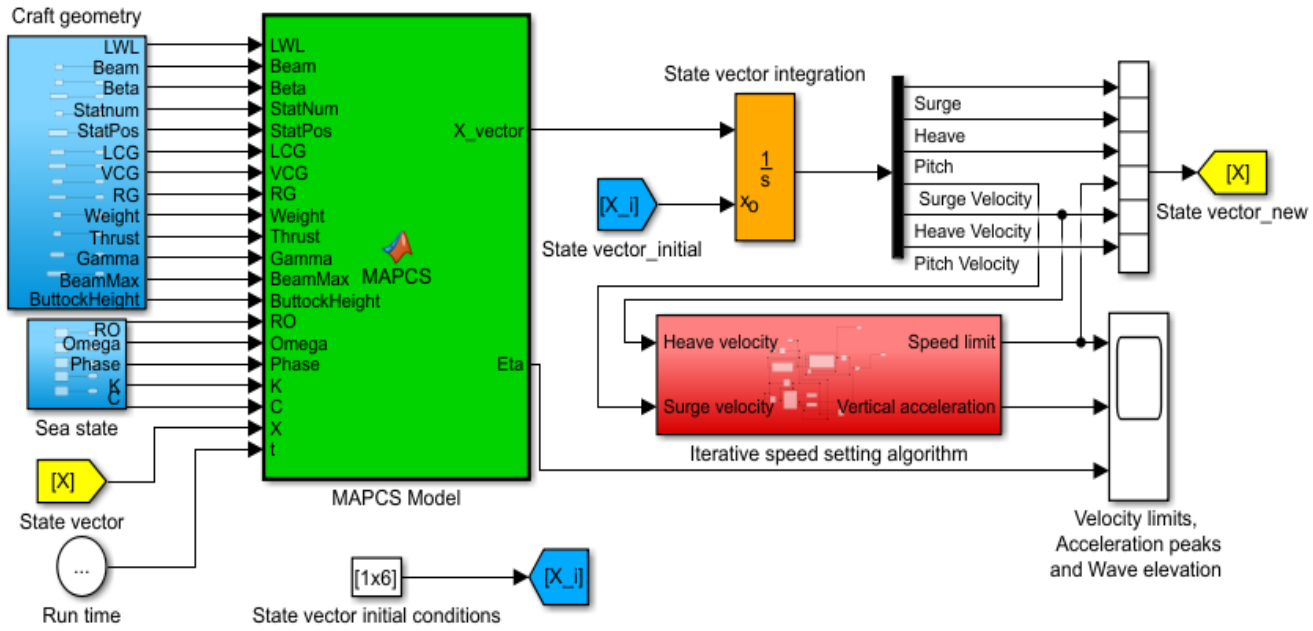

Figure 10. VSMS in Simulink environment

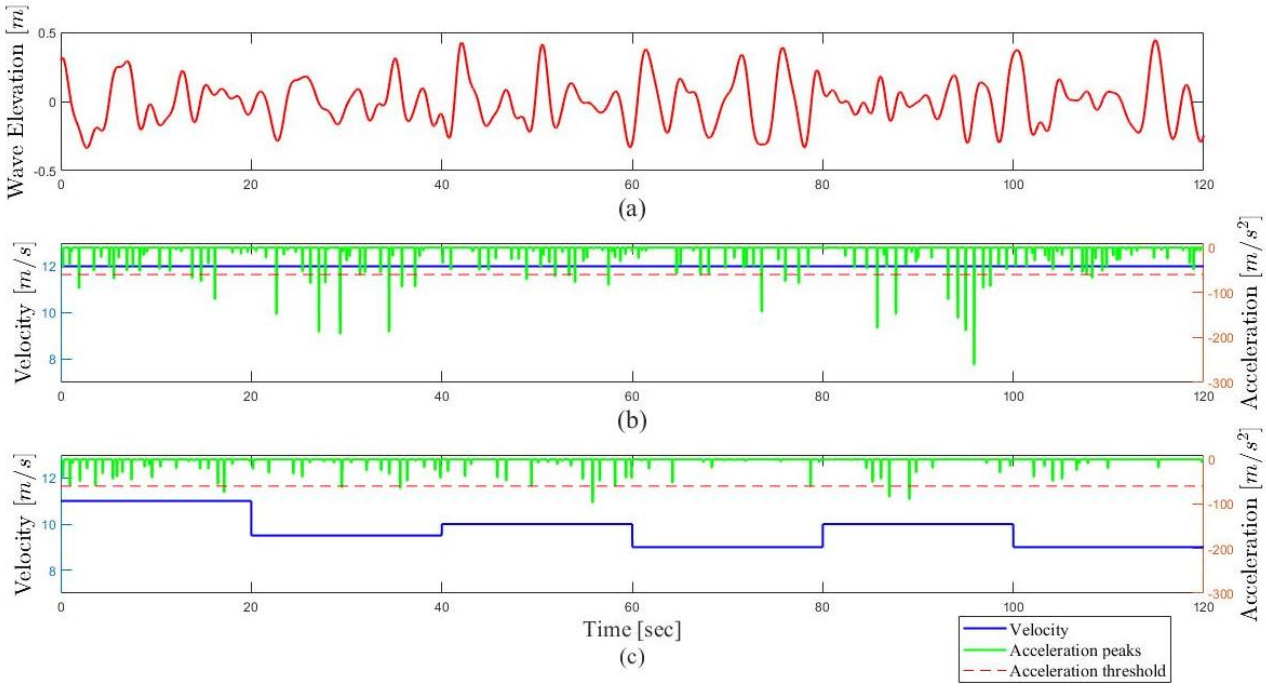

Figure 11. Comparison of the APC vertical acceleration responses with and without the VSMS for the same sea state

7. DISCUSSION AND CONCLUSIONS

From the obtained results, it was confirmed that the vision system presents a feasible method for estimating the incoming waves in undisturbed waters in front of a planing craft. The stereo camera employed in this study was further replaced by two separate, installed in a stereo configuration, industrial cameras equipped with zoom lenses enabling wave elevation reconstruction up to 50 [m] in front of the craft. This capability provided additional time for the VSMS computation process which is a progress towards real time usage of the system.

From the VSMS simulated results, by employing speed modulation as dictated by the system the vertical accelerations encountered by the craft are significantly reduced, while maximal possible speed is maintained implying the importance of a robust and reliable autonomous speed modulation system.

Future works will include improvement of all modules of the VSMS and integration of all in the APC to perform in real time.

8. ACKNOWLEDGEMENTS

This study was supported by the Leona M. and Harry B. Helmsley Charitable Trust, the Maurice Hatter Foundation, and the Paul Amir Foundation. Research at the University of Haifa was conducted at the Hatter Department of Marine Technologies in the Sub Sea Engineering Lab. The authors also thank the Coastal and Marine Engineering Research Institute, Haifa, Israel for providing real sea wave elevation data.

9. REFERENCES

1. ALLAKA, H. (2017) *Motion Assessment of Planing Craft in a Seaway*. Masters Thesis, University of Haifa.
2. ALLAKA, H. *et al.* (2018) *Vision-aided speed modulation system to enhance seaworthiness of autonomous planing crafts*. In Proceedings of 15th Workshop on Positioning, Navigation and Communications, WPNC, Bremen, Germany, 25-26 October, 2018, pp.1-6, DOI: 10.1109/WPNC.2018.8555758
3. ALLAKA, H. and GROPER, M. (2020) *Validation and verification of a planing craft motion prediction model based on experiments conducted on full-size crafts operating in real sea*. Journal of Marine Science and Technology. DOI: https://doi.org/10.1007/s00773-020-00709-6
4. ALLAKA, H. *et al.* (2019) *An Autonomous Speed Settin System to Enhance Operation of Unmanned Planing Crafts in a Seaway.* In Proceedings of the 6th International Conference on Ship and Offshore Technology, IIT Kharagpur, India, 7-8 November, 2019, pp. 189–196.
5. BERGAMASCO, F. *et al*. (2017) *WASS: An open-source pipeline for 3D stereo reconstruction of ocean waves.* Computers and Geosciences 107. pp.28-36. DOI: 10.1016/j.cageo.2017.07.001
6. BLAICH, M. *et al*. (2015) *Probabilistic collision avoidance for vessels*. IFAC-PapersOnLine, 28(16), pp.69–74. DOI: http://dx.doi.org/10.1016/j.ifacol.2015.10.260.

7. CAMERI. *Real Time Wave Measurements Haifa*. http://www.israports.co.il/SiteAssets/Waves/haifaw-ipa.html. (Accessed 16th March 2020)
8. CAMPBELL, S., ABU-TAIR, M. and NAEEM, W. (2013) *An automatic COLREGs-compliant obstacle avoidance system for an unmanned surface vehicle.* Proceedings of the Institution of Mechanical Engineers, Part M: Journal of Engineering for the Maritime Environment, 228(2), pp.108–121. DOI: https://doi.org/10.1177/1475090213498229.
9. CAMPBELL, S., NAEEM, W. and IRWIN, G.W. (2012) *A review on improving the autonomy of unmanned surface vehicles through intelligent collision avoidance manoeuvres*. Annual Reviews in Control, 36(2), pp.267–283.
10. CORGNATI, L. *et al*. (2015) *High resolution stereo imaging of sea waves for validation and optimization of wave modelling,* In Proceedings of OCEANS 2015 - MTS/IEEE, Genova, Genoa, May 2015, pp. 1-8. DOI: 10.1109/OCEANS-Genova.2015.7271382
11. EL-GAALY, T. *et al*. (2013) *Visual Obstacle Avoidance for Autonomous Watercraft using Smartphones.* In Proceedings of Autonomous Robots and Multirobot Systems workshop, ARMS, May, 2013.
12. FARBER, S. *et al*. (2018) *Estimating Sea State Using a Low Cost Buoy*. In Proceedings of IEEE International Conference on the Science of Electrical Engineering in Israel (ICSEE), Eilat, Israel, 12-14, Decemeber, 2018, pp. 1-5.
13. GARME, K. (2005) *Improved Time Domain Simulation of Planing Hulls in Waves by Correction of the Near-Transom Lift*. International Shipbuilding Progress, 52(3), pp.201–230.
14. HEIDARSSON, H.K. and SUKHATME, G.S. (2011) *Obstacle detection and avoidance for an autonomous surface vehicle using a profiling sonar.* In Proceedings of IEEE International Conference on Robotics and Automation, 9-13 May 2011, pp.731–736. DOI: 10.1109/ICRA.2011.5980509
15. HERMANN, D. *et al*. (2015) *Smart sensor based obstacle detection for high-speed unmanned surface vehicle.* IFAC-PapersOnLine, 28(16), pp.190–197.
16. JIAN CUI *et al*. (2017) *Wave height measurement using a short-range FMCW radar for unmanned surface craft.* In Proceedings of OCEANS 2015 - MTS/IEEE Washington, DC, USA, 19-22 October, 2015, pp.1–5. DOI: 10.23919/OCEANS.2015.7404392
17. LARSON, J., BRUCH, M. and EBKEN, J. (2006) *Autonomous navigation and obstacle avoidance for unmanned surface vehicles.* In Proceedings of SPIE - The International Society for Optical Engineering, June 2006, DOI: 10.1117/12.663798
18. MOE, S. and PETTERSEN, K.Y. (2017) *Set-Based line-of-sight (LOS) path following with collision avoidance for underactuated unmanned surface vessels under the influence of ocean currents.* In Proceedings of 1st Annual IEEE Conference on Control Technology and Applications, Mauna Lani, HI, USA, 27-30 August 2017, pp.241–248. DOI: 10.1109/CCTA.2017.8062470
19. Multi-Purpose USV Protector. *Rafael Advanced Defense Systems Ltd.* Available at: https://www.rafael.co.il/worlds/naval/usvs/ (Accessed 16th March 2020)
20. NIELSEN, U.D. *et al*. (2017) *New concepts for shipboard sea state estimation.*, In Proceedings of OCEANS 2015 - MTS/IEEE Washington, DC, USA, 19-22 October 2015, DOI: 10.23919/OCEANS.2015.7404386
21. NIELSEN, U.D. *et al*. (2016) *Evaluation of shipboard wave estimation techniques through model-scale experiments.* In Proceedings of OCEANS 2016 - Shanghai, 10-13 April 2016, DOI: 10.1109/OCEANSAP.2016.7485701
22. PAYNE, P.R. (1994) *Recent developments in "added-mass" planing theory*. Ocean Engineering, pp.257–309.
23. REVAUD, J. *et al*. (2015) *EpicFlow : Edge-Preserving Interpolation of Correspondences for Optical Flow.* In Proceedings of the IEEE Conference on Computer Vision and Pattern Recognition, June 2015, pp.1164–1172. DOI: 10.1109/CVPR.2015.7298720
24. ROSÉN, A. *et al*. (2017) *High-speed craft dynamics in waves : challenges and opportunities related to the current safety philosophy.* Proceedings of the 16th International Ship Stability Workshop, Belgrade, Serbia, 5-7 June 2017.
25. TRIPP, H. and DALTRY, R. (2017) *The Path to Real World Autonomy for Autonomous Surface Vehicles*. ASV Global 2017.
26. WANG, H. *et al*. (2011) *A vision-based obstacle detection system for Unmanned Surface Vehicle.In proceedings of* IEEE 5th International Conference on Robotics, Automation and Mechatronics (RAM), Qingdao, China, 17-19 September, 2011 pp.364–369. DOI: 10.1109/RAMECH.2011.6070512
27. ZARNICK, E.E. (1978) *A non-linear mathemathical model of motions of a planing boat in regular waves.* Tech. Rep. DTNSRDC-78/032, David Taylor Naval Ship Reasearch and Development Center, Bethesda, Md, USA.
28. ZHUANG, J.Y. *et al*. (2016) *Radar-based collision avoidance for unmanned surface vehicles*. China Ocean Engineering, 30(6), pp.867–883. DOI: https://doi.org/10.1007/s13344-016-0056-0

